ELSEVIER

Atmospheric Research 75 (2005) 323–345

ATMOSPHERIC RESEARCH

www.elsevier.com/locate/atmos

Approximation formulas for the microphysical properties of saline droplets

Edgar L Andreas*

U.S. Army Cold Regions Research and Engineering Laboratory, 72 Lyme Road, Hanover, New Hampshire 03755-1290, USA

Received 29 September 2004; accepted 2 February 2005

Abstract

Microphysical theory has proven essential for explaining sea spray's role in transferring heat and moisture across the air–sea interface. But large-scale models of air–sea interaction, among other applications, cannot afford full microphysical modules for computing spray droplet evolution and, thus, how rapidly these droplets exchange heat and moisture with their environment. Fortunately, because the temperature and radius of saline droplets evolve almost exponentially when properly scaled, it is possible to approximate a droplet's evolution with just four microphysical endpoints: its equilibrium temperature, T_{eq}; the e-folding time to reach that temperature, τ_T; its equilibrium radius, r_{eq}; and the e-folding time to reach that radius, τ_r.

Starting with microphysical theory, this paper derives quick approximation formulas for these microphysical quantities. These approximations are capable of treating saline droplets with initial radii between 0.5 and 500 μm that evolve under the following ambient conditions: initial droplet temperatures and air temperatures between 0 and 40 °C, ambient relative humidities between 75% and 99.5%, and initial droplet salinities between 1 and 40 psu.

Estimating T_{eq}, τ_T, and τ_r requires only one-step calculations; finding r_{eq} is done recursively using Newton's method. The approximations for T_{eq} and τ_T are quite good when compared to similar quantities derived from a full microphysical model; T_{eq} is accurate to within 0.02 °C, and τ_T is typically accurate to within 5%. The estimate for equilibrium radius r_{eq} is also usually within

* Tel.: +1 603 646 4436; fax: +1 603 646 4644.
E-mail address: eandreas@crrel.usace.army.mil.

0169-8095/$ - see front matter. Published by Elsevier B.V.
doi:10.1016/j.atmosres.2005.02.001

5% of the radius simulated with the full microphysical model. Finally, the estimate of radius e-folding time τ_r is accurate to within about 10% for typical oceanic conditions.
Published by Elsevier B.V.

Keywords: Aqueous solution droplets; Droplet evolution; Droplet radius; Droplet temperature; Cloud microphysics; Saline droplets; Sea spray

1. Introduction

Saline droplets do not evaporate to nothing. Unlike freshwater droplets from a lawn sprinkler, for example, a saline droplet that is exposed to evaporating conditions can reach a temperature and a radius at which it is still liquid but is in equilibrium with its environment. Such an equilibrium state exists for typical sea spray droplets when the relative humidity is 75% or higher (e.g., Twomey, 1953). For lower relative humidities, sea spray droplets give up all their liquid but leave behind a sea-salt particle.

Microphysical theory, such as described in Pruppacher and Klett (1978), does well in predicting the temperature and radius evolution of such saline droplets (El Golli et al., 1974; Andreas, 1989, 1990, 1995; Pattison and Belcher, 1999). But a full microphysical model to predict this evolution is complex and expensive to implement in larger models that require information on these droplet microphysical endpoints (e.g., Fairall et al., 1994; Edson et al., 1996; Kepert et al., 1999; Van Eijk et al., 2001; Andreas and Emanuel, 2001). Simplifications are needed. Fitzgerald's (1975) classic work shows some of the approximations that are possible when the goal is to predict the equilibrium radius of an aqueous solution droplet. Likewise, Andreas (1995, 1996) and Kepert (1996) devise approximations to predict the equilibrium temperature of sea spray droplets.

My particular reason for revisiting this topic, however, is because I want to make quick estimates of how sea spray droplets contribute to the air–sea fluxes of heat and moisture. Andreas (1992) parameterizes the sensible (Q_s) and latent (Q_L) heat fluxes near the sea surface that are mediated by all spray droplets with initial radius r_0 as

$$Q_s(r_0) = \rho_s c_{ps}\left(T_s - T_{eq}\right)\left[1 - \exp\left(-\tau_f/\tau_T\right)\right]\left(\frac{4\pi r_0^3}{3}\frac{dF}{dr_0}\right) \tag{1.1}$$

and

$$Q_L(r_0) = \rho_s L_v\left[1 - \left(\frac{r(\tau_f)}{r_0}\right)^3\right]\left(\frac{4\pi r_0^3}{3}\frac{dF}{dr_0}\right). \tag{1.2}$$

Andreas and DeCosmo (2002) integrate these quantities over all radii to get what they call the "nominal" spray fluxes. These are "nominal" fluxes because they must be multiplied by order-one tuning coefficients and combined to produce the actual spray fluxes.

In Eqs. (1.1) and (1.2), ρ_s is the seawater density; c_{ps}, the specific heat of seawater at constant pressure; T_s, the sea surface temperature and the initial temperature of the

droplets; and L_v, the latent heat of vaporization. The quantity dF/dr_0 is the spray generation function, the rate at which droplets of radius r_0 are produced at the sea surface (Andreas, 2002). Hence, $(4\pi r_0^3/3)dF/dr_0$ is the total volume flux at the sea surface of all droplets with initial radius r_0. The time scale τ_f in Eqs. (1.1) and (1.2), which is a function of r_0 and the wind speed, estimates the residence time of spray droplets in the air above the sea surface (Andreas, 1992).

The remaining variables in Eqs. (1.1) and (1.2) are the microphysical quantities that are my focus here. In Eq. (1.2), $r(\tau_f)$ is the spray droplet radius when the droplet re-enters the sea; Andreas (1992) approximates this as

$$r(\tau_f) = r_{eq} + (r_0 - r_{eq})\exp(-\tau_f/\tau_r). \tag{1.3}$$

Here, r_{eq} is the equilibrium radius of a droplet that started with radius r_0, and τ_r is the e-folding time to reach this radius. Similarly, in Eq. (1.1), T_{eq} is the equilibrium temperature of a droplet that started at radius r_0 and temperature T_s, and τ_T is the e-folding time to reach this temperature.

Andreas (1990) demonstrates that the temperature of a saline droplet at time t after its formation, $T(t)$, is well approximated by

$$\frac{T(t) - T_{eq}}{T_s - T_{eq}} = \exp(-t/\tau_T) \tag{1.4}$$

for t/τ_T up to at least 2.8. Thus, τ_T derives easily from

$$\frac{T(\tau_T) - T_{eq}}{T_s - T_{eq}} = e^{-1}. \tag{1.5}$$

Likewise, Eq. (1.3) derives from an approximate expression for the evolution of droplet radius (Andreas, 1989),

$$\frac{r(t) - r_{eq}}{r_0 - r_{eq}} = \exp(-t/\tau_r), \tag{1.6}$$

which is accurate up to at least $t/\tau_r = 1$. Therefore, the time constant τ_r satisfies

$$\frac{r(\tau_r) - r_{eq}}{r_0 - r_{eq}} = e^{-1}. \tag{1.7}$$

Fig. 1 depicts the temperature and radius evolution of a typical sea spray droplet and identifies the microphysical quantities of interest, T_{eq}, r_{eq}, τ_T, and τ_r. These quantities depend not only on initial radius r_0 but also on the ambient conditions: air temperature (T_a), sea surface temperature (T_s) and salinity (S), relative humidity (RH), and barometric pressure.

Fig. 1 is based on calculations with a full microphysical model (i.e., Andreas, 1989, 1990, 1992). But in light of Eqs. (1.4) and (1.6), the microphysical endpoints T_{eq}, r_{eq}, τ_T, and τ_r may be sufficient to characterize droplet evolution for some applications. Therefore, here I develop approximation formulas for these microphysical quantities. Kepert (1996) and Andreas (1996) have already given equations to predict T_{eq}; I, nevertheless, repeat these here for completeness and as a springboard for developing the other formulas.

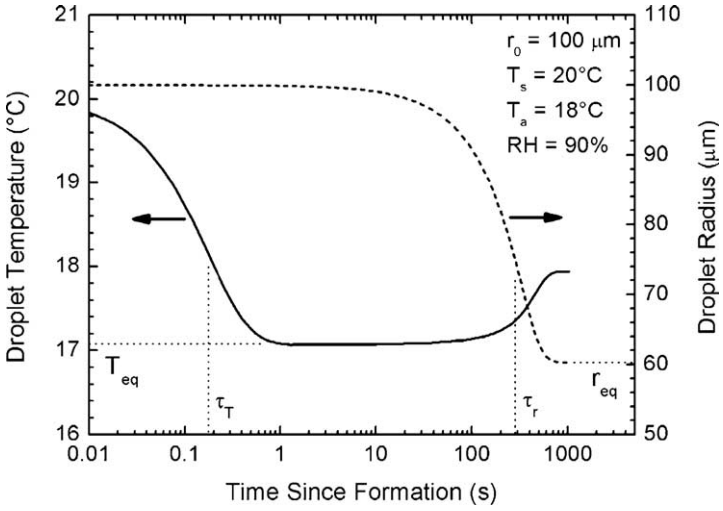

Fig. 1. Typical temperature and radius evolution of a sea spray droplet that started with a radius r_0 of 100 μm and with temperature T_s of 20 °C. Air temperature (T_a) is 18 °C, relative humidity (RH) is 90%, initial droplet salinity is 34 psu, and barometric pressure is 1000 mbar. The microphysical properties of this droplet, T_{eq}, r_{eq}, τ_T and τ_r, are also labeled.

Fitzgerald's (1975) equations for r_{eq} are appropriate for a host of solutes, including NaCl. But for salt water, at least, his equations predict equilibrium radii that do not agree especially well with predictions from my microphysical model. Hence, I describe a new method to predict r_{eq}. Finally, I also develop methods to predict τ_T and τ_r quickly.

2. Microphysical background

Pruppacher and Klett (1978) develop equations to predict the radius and temperature evolution of aqueous solution droplets on the basis of microphysical theory. Andreas (1989, 1990, 1992, 1995, 1996) adapted these equations to sea spray droplets with initial radii ranging from 0.1 to 500 μm and assumed the solute was simply NaCl. Since I take these equations as bases for the approximation formulas, I briefly review them.

2.1. Radius evolution

Pruppacher and Klett's (1978, Eq. (13-28)) equation for the evolution of a saline droplet with instantaneous radius r is (also Andreas, 1989)

$$\frac{dr}{dt} = \frac{[(f-1)-y]r^{-1}}{\dfrac{\rho_s R T_a}{D'_w M_w e_{sat}(T_a)} + \dfrac{\rho_s L_v}{k'_a T_a}\left(\dfrac{L_v M_w}{R T_a} - 1\right)}. \tag{2.1}$$

Here, f (=RH/100) is the fractional ambient relative humidity; T_a, the ambient air temperature in Kelvin; R, the universal gas constant; M_w, the molecular weight of water;

and $e_{sat}(T_a)$, the saturation vapor pressure for a planar surface of pure water at temperature T_a (e.g., Buck, 1981).

Also in Eq. (2.1), D'_w and k'_a are values of the usual molecular diffusivity for water vapor in air (D_w) and the thermal conductivity of air (k_a) that are modified for the noncontinuum behavior of air and water vapor molecules around very small droplets. Pruppacher and Klett (1978, Eqs. (13-13) and (13-20); also Andreas, 1995) give the equations for D'_w and k'_a that I use here. Andreas (1989) shows that k'_a is not much different from k_a when r_0 is greater than 1 μm, but D'_w is significantly smaller than D_w for r_0 values up to 100 μm.

Lastly in Eq. (2.1),

$$y = \frac{2M_w\sigma_s}{RT_a\rho_w r} - \frac{v\Phi_s m_s(M_w/M_s)}{(4\pi\rho_s r^3/3) - m_s}. \tag{2.2}$$

Here, ρ_w is the density of pure water; m_s, the mass of salt in the droplet (a constant); M_s, the molecular weight of sodium chloride; and v, the number of ions into which a sodium chloride molecule dissociates. Also in Eq. (2.2), σ_s is the surface tension of a flat water surface with the same temperature and salinity as the droplet. I compute this from Eq. (5-19) in Pruppacher and Klett (1978).

Finally in Eq. (2.2), Φ_s is the practical osmotic coefficient. Andreas (1989) derives the following functional form for this when the solute is NaCl:

$$\Phi_s = 0.9270 - 2.164\times10^{-2}m + 3.486\times10^{-2}m^2 - 5.956\times10^{-3}m^3 + 3.911\times10^{-4}m^4. \tag{2.3}$$

Here, Φ_s is dimensionless; and this expression is accurate for molality m between 0 and 6 mol kg^{-1}, where

$$m = \frac{m_s}{M_w m_w}. \tag{2.4}$$

and m_w is the mass of water in the droplet.

Note that if S is the surface salinity of the seawater (in psu), we can find m_s for use in Eqs. (2.2) and (2.4) from the definition of salinity,

$$s = \frac{m_s}{m_{w0} + m_s}, \tag{2.5}$$

where m_{w0} is the initial mass of pure water in the droplet and s ($=S/1000$) is the fractional salinity. In turn,

$$\frac{m_s}{m_{w0}} = \frac{s}{1-s}. \tag{2.6}$$

Then, as an approximation for use in Eq. (2.2),

$$m_s \simeq \frac{4}{3}\pi\rho_w r_0^3\left(\frac{s}{1-s}\right). \tag{2.7}$$

In practice, the variable y simply models how curvature (the Kelvin effect) and dissolved salt affect the saturation vapor pressure at the surface of an aqueous solution droplet. That is, if $e_{sat}(T)$ is the saturation vapor pressure of a planar surface of pure water at temperature T and if $e_{sat}(T, r, m)$ is the saturation vapor pressure at the surface of a droplet with temperature T, molality m, and radius r (e.g., Pruppacher and Klett, 1978, Eq. (6-26a)),

$$e_{sat}(T, r, m) = e_{sat}(T)\exp(y). \tag{2.8}$$

2.2. Temperature evolution

I also start with Pruppacher and Klett's (1978, Eq. (13-64)) equation for the temperature evolution of a solution droplet:

$$\frac{d}{dt}(T_a - T) = \frac{-3}{\rho_s c_{ps} r^2}\left[k'_a(T_a - T) + L_v D'_w(\rho_v - \rho_{vr})\right]. \tag{2.9}$$

Here, T is the instantaneous droplet temperature, and the droplet is assumed to be well mixed (i.e., of uniform temperature; Andreas, 1990). Variable ρ_v denotes water vapor density such that ρ_v is the ambient vapor density and, in my nomenclature, is

$$\rho_v = \frac{f M_w e_{sat}(T_a)}{R T_a}, \tag{2.10}$$

which gives ρ_v in kg m^{-3} when e_{sat} is computed in Pascal. Likewise, ρ_{vr} is the (saturation) vapor density at the surface of the droplet,

$$\rho_{vr} = \frac{M_w e_{sat}(T)}{RT}\exp(y). \tag{2.11}$$

Eq. (2.9) simply states that a droplet changes temperature as a consequence of two processes: heat diffusion and vapor diffusion at its surface.

Pruppacher and Klett (1978, Eqs. (13-50) and (13-64)) include ventilation coefficients in their expressions for droplet evolution—my Eqs. (2.1) and (2.9) (cf. Fairall et al., 1994; Edson and Fairall, 1994; Kepert et al., 1999). I ignore these terms here since they have not seemed necessary when I compared model calculations with data (Andreas, 1990). Furthermore, the small droplets that I consider respond almost immediately to turbulent eddies (Andreas, 2004) and, therefore, rarely have a speed that differs much from the local flow speed. That is, they are not strongly "ventilated".

2.3. Implications

Because Eqs. (2.1) and (2.9) are coupled by the presence of $T(t)$ and $r(t)$ in both equations, a full solution for the evolution of a spray droplet must solve both equations simultaneously. Andreas (1989) gives the numerical details for such a solution, and this is the process I followed to produce Fig. 1. I will refer to such calculations as a *full* microphysical simulation.

Fig. 1 is typical of many similar computational runs that I have made in the sense that all these show that temperature evolution and radius evolution are nearly decoupled (cf. Andreas, 1990, 1992; Andreas and DeCosmo, 1999). In other words, a droplet falls to its equilibrium temperature T_{eq} before much water has evaporated. Then the evaporation to its equilibrium radius r_{eq} occurs, largely, while the droplet is at constant temperature T_{eq}. The time scales that characterize these two processes, τ_T and τ_r (see Fig. 1), therefore always differ by three orders of magnitude: thermal evolution is very quick; radius evolution is much slower. This decoupling also means that the relative humidity has little influence on T_{eq} or τ_T, while the sea surface temperature has little influence on r_{eq} or τ_r since the droplet is at T_{eq} for most of its evaporation.

I will invoke this decoupling to deduce approximation formulas for T_{eq}, r_{eq}, τ_T, and τ_r.

3. Droplet equilibrium temperature, T_{eq}

Many presume that the equilibrium temperature, T_{eq}, of a sea spray droplet is the wet-bulb temperature, T_{wet} (cf. Kinzer and Gunn, 1951; Fairall et al., 1994; Lighthill, 1999; Bao et al., 2000). Andreas (1995) demonstrates, however, that, because a seawater droplet is saline and has a highly curved surface, T_{eq} can differ significantly from T_{wet}, especially for droplets with radii less than 10 μm. That is, Eq. (2.8) shows that the vapor pressure at the surface of a droplet depends not only on $e_{sat}(T)$–which is the key moisture variable in the definition of the wet-bulb temperature–but also on droplet size and salinity.

Kepert (1996) therefore devised a quick method to estimate T_{eq} from the microphysical equations given above. Andreas (1996) modified Kepert's method slightly to make it compatible with my specific implementation of the microphysical equations. That prediction equation is

$$\left\{\frac{\beta}{T_a^2}\left[\frac{\alpha^2}{2}-\alpha\left(\frac{2T_a+b-273.15}{T_a+b-273.15}\right)+1\right]\exp(y)\right\}\Delta T^2 + \left[1+\frac{\beta}{T_a}(\alpha-1)\exp(y)\right]\Delta T-\beta[f-\exp(y)]=0. \tag{3.1}$$

Here,

$$\alpha=\frac{abT_a}{(b+T_a-273.15)^2} \tag{3.2}$$

and

$$\beta=\frac{e_{sat}(T_a)}{T_a}\,\frac{L_v M_w D'_w}{Rk'_a}, \tag{3.3}$$

where $a=17.502$ and $b=240.97$ °C.

Eq. (3.1) is a quadratic in ΔT, where

$$\Delta T=T_{eq,est}-T_a, \tag{3.4}$$

$T_{eq,est}$ is an estimate of T_{eq}, and both $T_{eq,est}$ and T_a are in Kelvin. The solution therefore involves evaluating the coefficients in Eq. (3.1) at the droplet's initial conditions–the radius is r_0, temperature is T_s, and salinity S is the surface salinity of the ocean–and then solving for ΔT.

Kepert (1996) and Andreas (1996) show that estimates of T_{eq} based on this procedure are within 0.02 °C of the equilibrium temperature that results from integrating the full microphysical equations [i.e., Eqs. (2.1) and (2.9)] for all droplets with initial radii from 0.5 to 500 μm, for air temperatures from 0 to 30 °C, and for salinities from 0 to 40 psu. The solution is likely accurate for conditions beyond these ranges, but these are the conditions for which we tested it.

Eq. (3.1) is not, however, valid for all relative humidities that exist over the ocean. Dry sea salt particles deliquesce (change from dry particles to aqueous droplets) as the relative humidity rises through 75% (Twomey, 1953; Pruppacher and Klett, 1978, Table 4-3). Likewise, seawater droplets evolve into dry sea salt particles when placed in an environment with a relative humidity less than 75%. Therefore, Eq. (3.1) is not appropriate when the ambient relative humidity is less than 75%. Kepert (1996) and Andreas (1996) discuss this issue in more detail.

If a spray droplet undergoes this transition to a sea salt particle, its final temperature will simply be T_a, the air temperature. We can also estimate its final radius as the effective dry radius, r_d, from

$$r_d = \left(\frac{3 m_s}{4\pi \rho_{NaCl}} \right)^{1/3}, \tag{3.5}$$

where ρ_{NaCl} is the density of sodium chloride, and m_s comes from Eq. (2.7).

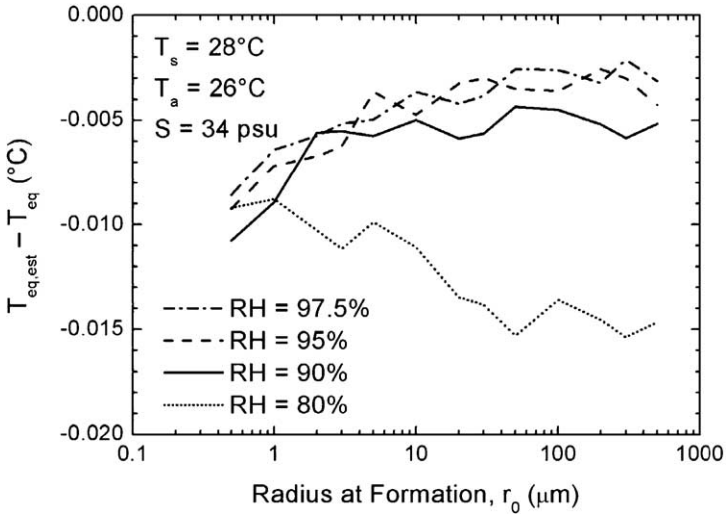

Fig. 2. A comparison of two estimates of the droplet equilibrium temperature: one (T_{eq}) is based on the full microphysical equations and is assumed to be more accurate; the other ($T_{eq,est}$) is a quick estimate based on Eqs. (3.1)–(3.4). Here, sea surface temperature (T_s) is 28 °C, air temperature (T_a) is 26 °C, sea surface salinity (S) is 34 psu, and the relative humidity (RH) ranges from 80% to 97.5%. Barometric pressure is assumed to be 1000 mbar.

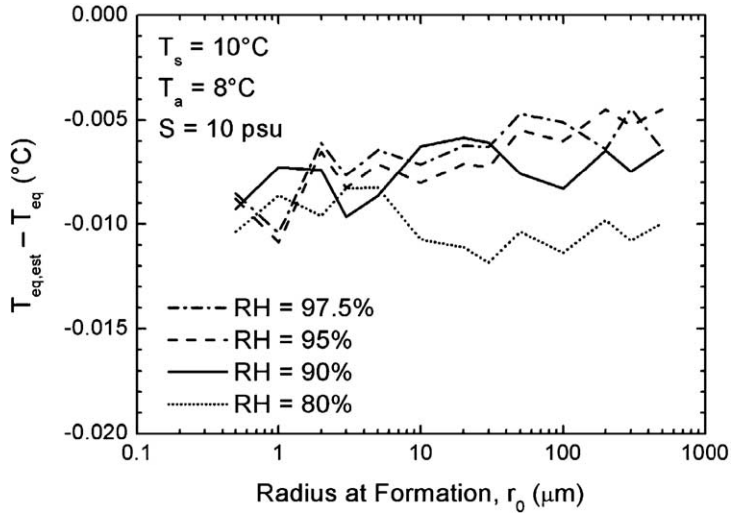

Fig. 3. As in Fig. 2; but here, water temperature is 10 °C, air temperature is 8 °C, and surface salinity is 10 psu.

Figs. 2 and 3 show sample calculations of the droplet equilibrium temperature based on Eqs. (3.1)–(3.4). Fig. 2 depicts typical conditions over the tropical ocean; Fig. 3 is for lower temperature and lower salinity. In both plots, though, the quick estimate of equilibrium temperature, $T_{eq,est}$, is always within about 0.015 °C of the equilibrium temperature computed with my full microphysical model (denoted T_{eq}).

Andreas (1996) shows similar plots for other conditions; and these, too, suggest that $T_{eq,est}$ is biased low compared to T_{eq}. On the other hand, Kepert's (1996) similar plots always show his particular estimate of $T_{eq,est}$ to be greater than T_{eq}. Andreas (1996), however, repeats some of Kepert's calculations and still finds $T_{eq,est} - T_{eq}$ to be negative. I believe we must be using slightly different parameterizations in our full microphysical models. Nevertheless, the conclusion remains that Eqs. (3.1)–(3.4) yield estimates of the droplet equilibrium temperature that are within a few hundredths of a degree of a much more computationally intensive estimate based on a full microphysical simulation.

4. Droplet temperature time constant, τ_T

Pruppacher and Klett (1978, pp. 446–447) estimate the temperature e-folding time τ_T starting from Eq. (2.9) (also Edson and Fairall, 1994). Here, I present a slightly modified version of their derivation that is more compatible with my full microphysical model.

Because the droplet radius changes very little over time τ_T (see Fig. 1), ρ_{vr} in Eq. (2.9) is essentially a function only of droplet temperature T during the initial stages of droplet evolution [see Eqs. (2.11) and (2.8)]. Furthermore, this same observation argues that $L_v D'_w(\rho_v - \rho_{vr})$ is a small term in Eq. (2.9). We can therefore approximate

$$\rho_{vr} \simeq \rho_{v,sat}(T), \tag{4.1}$$

where $\rho_{v,sat}(T)$ is Eq. (2.11) with y set to zero. This approximation basically means that we are ignoring the effects of droplet curvature and salinity to estimate the saturation vapor density at the droplet's surface. I will show later, however, that this approximation does not degrade our ability to predict τ_T for small droplets or for a wide range of salinities—again, because evaporation plays little role in determining how droplet temperature evolves toward T_{eq}.

With these approximations, the water vapor term in Eq. (2.9) becomes

$$\rho_v - \rho_{vr}(T) \simeq -\rho_{v,sat}(T_a)\left[1 - \frac{\rho_v}{\rho_{v,sat}(T_a)}\right] + \left[\rho_{v,sat}(T_a) - \rho_{v,sat}(T)\right]. \tag{4.2}$$

Here, we recognize $\rho_v/\rho_{v,sat}(T)$ as the fractional relative humidity, f.

Substituting Eq. (4.2) into Eq. (2.9) yields

$$\frac{d}{dt}(T_a - T) = \frac{-3(T_a - T)}{\rho_s c_{ps} r^2}\left[k'_a + \frac{L_v D'_w\left[\rho_{v,sat}(T_a) - \rho_{v,sat}(T)\right]}{T_a - T}\right] + \frac{3L_v D'_w(1-f)\rho_{v,sat}(T_a)}{\rho_s c_{ps} r^2}. \tag{4.3}$$

If we approximate

$$\frac{\rho_{v,sat}(T_a) - \rho_{v,sat}(T)}{T_a - T} \simeq \left.\frac{\partial \rho_{v,sat}}{\partial T}\right|_{T_a} \tag{4.4}$$

and invoke the observation from Fig. 1 that r changes negligibly while droplet temperature falls to T_{eq}, we can further approximate Eq. (4.3) as

$$\frac{d}{dt}[T_a - T(t)] = -A[T_a - T(t)] + B. \tag{4.5}$$

Here,

$$A = \frac{3}{\rho_s c_{ps} r_0^2}\left(k'_a + L_v D'_w \left.\frac{\partial \rho_{v,sat}}{\partial T}\right|_{T_a}\right) \tag{4.6}$$

and

$$B = \frac{3L_v D'_w(1-f)\rho_{v,sat}(T_a)}{\rho_s c_{ps} r_0^2}. \tag{4.7}$$

That is, r in Eq. (4.3) is r_0, and we evaluate L_v at T_s and k'_a and D'_w at r_0 and T_s. Lastly, in Eq. (4.5), I compute $\partial\rho_{v,sat}/\partial T|_{T_a}$ from (e.g., Andreas and Cash, 1996)

$$\left.\frac{\partial \rho_{v,sat}}{\partial T}\right|_{T_a} = \rho_{v,sat}(T_a)\left[\frac{ab}{(b + T_a - 273.15)^2} - \frac{1}{T_a}\right], \tag{4.8}$$

where T_a is still in Kelvin.

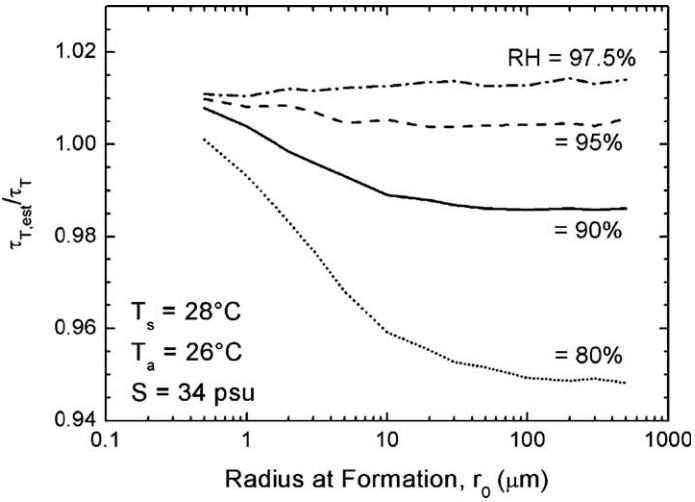

Fig. 4. A comparison of two estimates of a spray droplet's temperature e-folding time. One estimate (τ_T) is based on my full microphysical model; the other ($\tau_{T,est}$) is a quick estimate based on Eq. (4.11). Ambient conditions here are as in Fig. 2.

With A and B constants for the given conditions, Eq. (4.5) has the solution

$$T_a - T(t) = (T_a - T_s)\exp(-At) + \frac{B}{A}[1 - \exp(-At)]. \tag{4.9}$$

As t approaches infinity here, $T(t)$ approaches T_{eq}; therefore, within this approximation, $T_a - B/A$ is another estimate of T_{eq}. Consequently, we can reduce Eq. (4.9) to

$$\frac{T(t) - T_{eq}}{T_s - T_{eq}} = \exp(-At). \tag{4.10}$$

Compare this with Eq. (1.4), which is the equation that defines τ_T. Clearly,

$$\tau_{T,est} = \frac{1}{A} = \frac{\rho_s c_{ps} r_0^2}{3\left(k'_a + L_v D'_w \left.\frac{\partial \rho_{v,sat}}{\partial T}\right|_{T_a}\right)}. \tag{4.11}$$

Figs. 4 and 5 compare estimate of the temperature e-folding time based on Eq. (4.11) with estimates based on my full microphysical model (denoted τ_T) for the same ambient conditions depicted in Figs. 2 and 3. For the cases shown, which are typical of other ambient conditions, $\tau_{T,est}$ is within 5% of τ_T and, for typical oceanic conditions, is usually much closer to τ_T.

5. Droplet equilibrium radius, r_{eq}

Fitzgerald (1975) derived formulas to approximate the equilibrium radius r_{eq} of aqueous solution droplets for a variety of solutes. Andreas (1989) showed, however, that, when the solute is NaCl, Fitzgerald's estimates of r_{eq} differ appreciably from estimates based on full

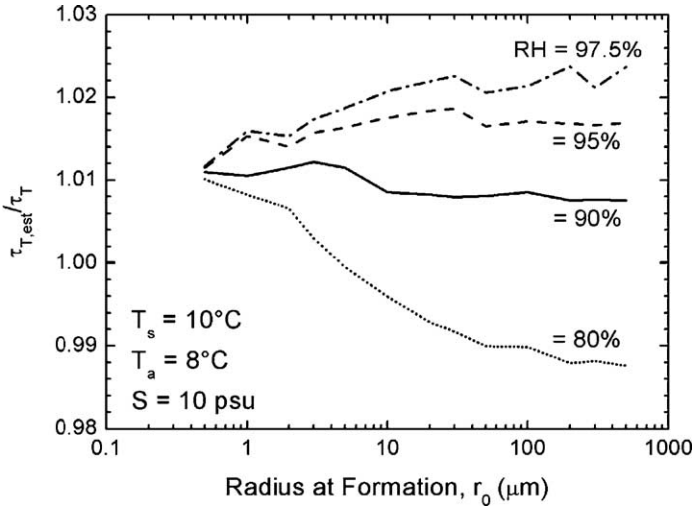

Fig. 5. As in Fig. 4; but here, ambient conditions are as in Fig. 3.

microphysical calculations. Therefore, I derive here a new method for estimating r_{eq} that is more compatible with a modern microphysical model of droplet evolution.

My criterion for a droplet to be at its equilibrium radius is that its radius is no longer changing with time. In other words, in the radius evolution equations, Eq. (2.1), $dr/dt = 0$. Therefore, the equilibrium radius satisfies

$$(f-1) - y(r_{eq}) = 0, \tag{5.1}$$

where Eq. (2.2) gives y as a function of radius and other variables.

By defining the function

$$g(r) = (f-1) - y(r), \tag{5.2}$$

we can use Newton's method to find r_{eq}. The recursion relation is

$$r_{k+1} = r_k - \frac{g(r_k)}{\partial g/\partial r|_{r_k}}, \tag{5.3}$$

where r_k is the kth estimate of r_{eq} in the iterative solution.

For completeness, let me write down $\partial g/\partial r$, which is

$$\frac{\partial g}{\partial r} = \frac{2M_w\sigma_s}{RT_a\rho_w r^2} - \frac{v\Phi_s m_s(M_w/M_s)}{(4\pi\rho_s r^3/3) - m_s}\left(4\pi r^2\rho_s\right). \tag{5.4}$$

Note that σ_s, Φ_s, and ρ_s here all are functions of radius because, as the droplet evaporates, the droplet's salinity increases. Andreas (1989) gives equations for σ_s and ρ_s as functions of salinity and temperature; but these come right out of Pruppacher and Klett (1978). I evaluate both σ_s and ρ_s at T_{eq}. Eq. (2.3) shows how to compute Φ_s.

Figs. 6 and 7 compare sample calculations of the equilibrium radius estimated from Eqs. (5.1)–(5.4) (i.e., $r_{eq,est}$) with estimates from the full microphysical model (designated

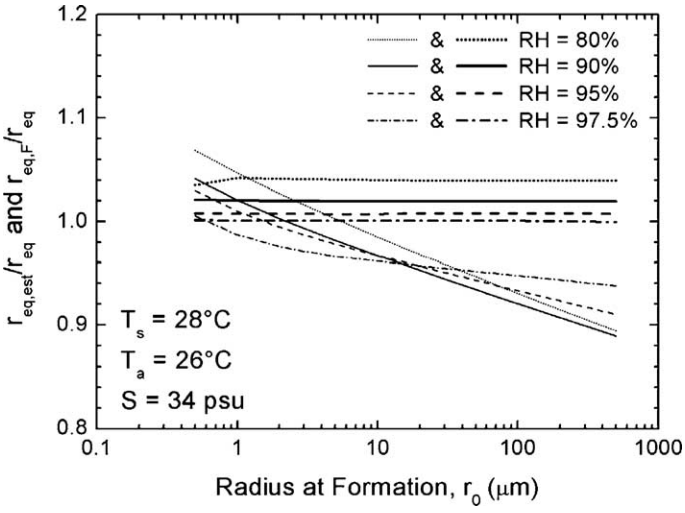

Fig. 6. Two quick estimates of the equilibrium radius of a saline water droplet are compared with estimates based on my full microphysical model (r_{eq}). The quick estimates derive from Eqs. (5.1)–(5.4) ($r_{eq,est}$, thick lines) and from Fitzgerald's (1975) algorithm ($r_{eq,F}$, thin lines). Ambient conditions here are as in Fig. 2.

r_{eq}). Ambient conditions are the same as in Figs. 2 and 3. To reiterate the statement I made earlier that Fitzgerald's (1975) approximation methods do not agree with my full microphysical calculations, I also plot in Figs. 6 and 7 estimates of r_{eq} based on his algorithm (i.e., $r_{eq,F}$).

The results depicted in Figs. 6 and 7 show that my quick estimates of r_{eq} (i.e., $r_{eq,est}$) agree very well with estimates derived from a full microphysical simulation of droplet evolution: $r_{eq,est}$ is typically within 4% of r_{eq}.

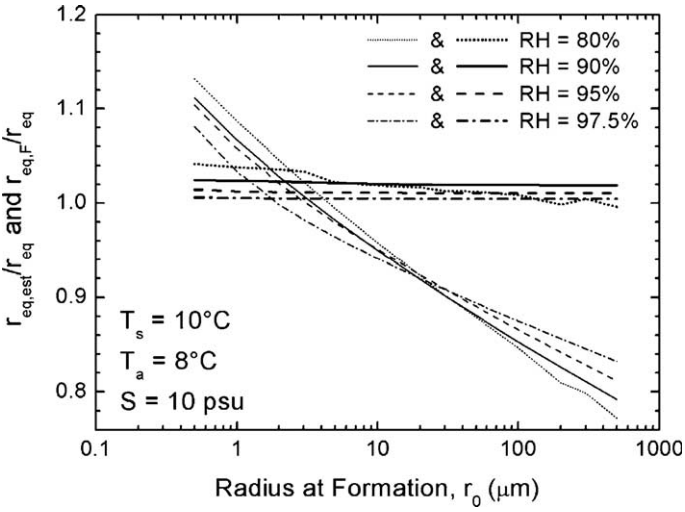

Fig. 7. As in Fig. 6; but here, ambient conditions are as in Fig. 3.

Fitzgerald's (1975) algorithm differs markedly in Figs. 6 and 7 from both my full microphysical model and from my quick estimate of r_{eq}. Admittedly, I am sometimes using his algorithm beyond the size and humidity ranges for which he developed it. He states that it is appropriate for droplets with initial radii between about 0.2 and 12 μm and for relative humidities of at least 81%. But even within these ranges, Fitzgerald's estimates are higher for small droplets and lower for larger droplets than r_{eq} values based on my full microphysical model. Plots in Andreas (1989) show this same behavior. I, of course, believe my modern model is more correct than Fitzgerald's algorithm, but I know of no independent confirmation of this conclusion. Nevertheless, because droplets with initial radii up to 500 μm are important in the spray latent heat equation, Eq. (1.2) (Andreas, 1992), I need a better estimate of r_{eq} for these large droplets than Fitzgerald's algorithm can provide.

6. Droplet radius time constant, τ_r

The radius e-folding time τ_r, as defined by Eq. (1.7), has proven to be the most difficult of the four microphysical endpoints to estimate quickly. I have tried several approaches and present here the most accurate that I have found; this approach, however, still produces estimates of τ_r that, for some conditions, differ by several tens of percent from τ_r values based on full microphysical simulations.

For t/τ_r up to 1, Eq. (1.6) suggests that the function

$$h(t) \equiv \ln\left[\frac{r(t) - r_{eq}}{r_0 - r_{eq}}\right] \tag{6.1}$$

is approximately linear in t. I therefore model $h(t)$ around time zero with a second-order Taylor series:

$$h(t) = h(0) + t\left.\frac{dh}{dt}\right|_{t=0} + \frac{1}{2}t^2\left.\frac{d^2h}{dt^2}\right|_{t=0} \tag{6.2}$$

for $t \le \tau_r$.

Because $r(0)=r_0$ by definition, $h(0)=0$. Further, from Eq. (6.1),

$$\frac{dh}{dt} = \frac{1}{r(t) - r_{eq}}\frac{dr}{dt}. \tag{6.3}$$

Hence,

$$\left.\frac{dh}{dt}\right|_{t=0} = \frac{1}{r_0 - r_{eq}}\left.\frac{dr}{dt}\right|_{r_0}, \tag{6.4}$$

where I can easily evaluate $dr/dt|_{r_0}$ from Eq. (2.1).

Likewise, from Eq. (6.3),

$$\frac{d^2h}{dt^2} = \frac{1}{r(t) - r_{eq}}\frac{d^2r}{dt^2} - \frac{1}{\left[r(t) - r_{eq}\right]^2}\left(\frac{dr}{dt}\right)^2. \tag{6.5}$$

Consequently, in Eq. (6.2),

$$\left.\frac{d^2h}{dt^2}\right|_{t=0} = \frac{1}{r_0 - r_{eq}} \left.\frac{d^2r}{dt^2}\right|_{r_0} - \frac{1}{(r_0 - r_{eq})^2} \left(\left.\frac{dr}{dt}\right|_{r_0}\right)^2, \tag{6.6}$$

where $d^2r/dt^2|_{r_0}$ also comes from Eq. (2.1).

I want to determine τ_r from Eq. (6.2). From Eqs. (1.6) and (6.1), we see that $h(\tau_r) = -1$. Hence, with Eqs. (6.4) and (6.6), Eq. (6.2) becomes

$$0 = 1 + \left[\frac{1}{r_0 - r_{eq}} \left.\frac{dr}{dt}\right|_{r_0}\right]\tau_r + \frac{1}{2}\left[\frac{1}{r_0 - r_{eq}} \left.\frac{d^2r}{dt^2}\right|_{r_0} - \frac{1}{(r_0 - r_{eq})^2}\left(\left.\frac{dr}{dt}\right|_{r_0}\right)^2\right]\tau_r^2 \tag{6.7}$$

when it is evaluated at τ_r. The quadratic formula then gives

$$\tau_{r,est} = \frac{-\left.\frac{dr}{dt}\right|_{r_0} - \left[3\left(\left.\frac{dr}{dt}\right|_{r_0}\right)^2 - 2(r_0 - r_{eq})^2 \left.\frac{d^2r}{dt^2}\right|_{r_0}\right]^{1/2}}{\left.\frac{d^2r}{dt^2}\right|_{r_0} - \frac{1}{r_0 - r_{eq}}\left(\left.\frac{dr}{dt}\right|_{r_0}\right)^2}. \tag{6.8}$$

Here, I have taken the negative sign on the square root term in the numerator because the denominator is always negative for evaporating droplets. To be consistent with my theme of developing methods to compute the microphysical endpoints quickly, I compute r_{eq} for use in Eq. (6.8) from the algorithm in Section 5.

Figs. 8 and 9 compare estimates of the radius e-folding time computed with Eq. (6.8) with values from my full microphysical model (denoted τ_r) for the same ambient

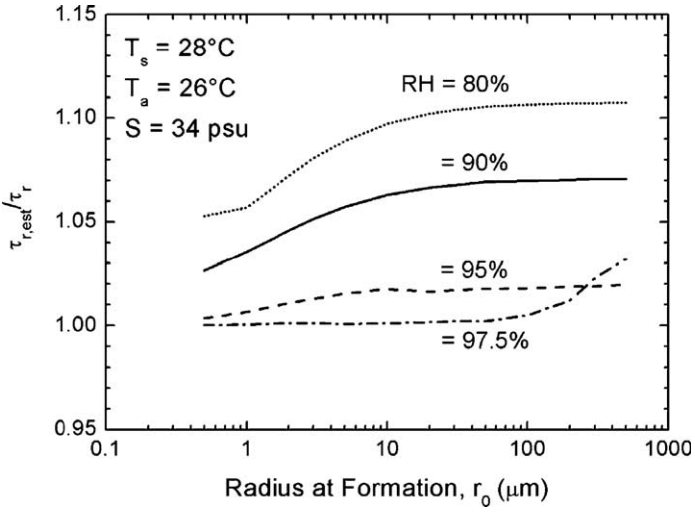

Fig. 8. My quick estimate of the radius e-folding time from Eq. (6.8) (i.e., $\tau_{r,est}$) is compared with the e-folding time computed with the full microphysical model (i.e., τ_r). Ambient conditions are as in Fig. 2.

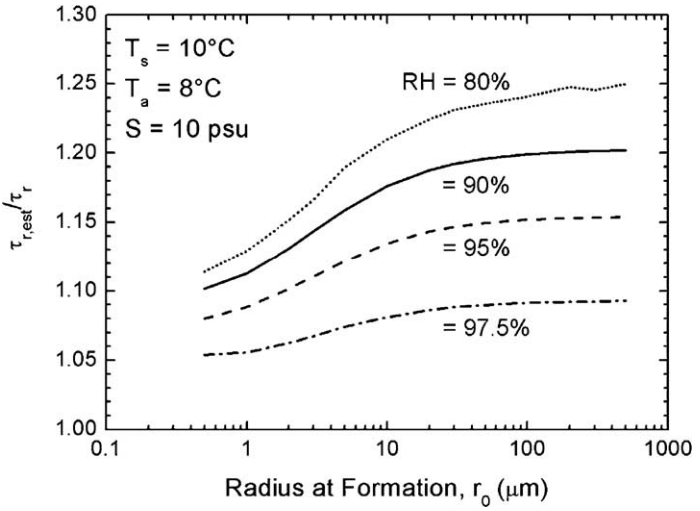

Fig. 9. As in Fig. 8; but here, ambient conditions are as in Fig. 3.

conditions as in Figs. 2 and 3. The estimates of τ_r here based on Eq. (6.8) are not as good, in general, as my quick estimates of the other microphysical endpoints: in these figures, $\tau_{r,est}$ differs from τ_r by as much as 25%. But for typical oceanic conditions–that is, for a sea surface salinity near 34 psu–the quick estimate seems to be fairly good: in Fig. 8, $\tau_{r,est}$ is always within 11% of τ_r for the relative humidities depicted.

I suspect that the relatively poor performance of Eq. (6.8) for low salinity results because my algorithm must evaluate dr/dt and d^2r/dt^2 in Eq. (6.8) at r_0, which is much larger than r_{eq} when the salinity is low. In other words, a truncated Taylor series expansion around $t=0$, Eq. (6.2), is not as accurate when the droplet radius at equilibrium is a lot smaller than the initial radius.

In high humidities, when spray droplets grow rather than evaporate, the square root term in the numerator of Eq. (6.8) can have a negative argument. Eq. (6.8) therefore does not have a real solution. To work around this problem, I test to make sure that the argument within the square root is positive. If it is not, I use the method described next to estimate τ_r.

Notice from Eq. (1.6) that

$$\frac{dr}{dt} = -\frac{r_0 - r_{eq}}{\tau_r}\exp(-t/\tau_r). \tag{6.9}$$

Hence, at $t=0$, when $r(t)=r_0$,

$$\tau_{r1} = -\frac{r_0 - r_{eq}}{dr/dt|_{r_0}} \tag{6.10}$$

is another estimate of the radius e-folding time. I denote it τ_{r1} because Eq. (6.10) is equivalent to a first-order Taylor series [i.e., see Eq. (6.7)]. Of course, $dr/dt|_{r_0}$ must again come from Eq. (2.1).

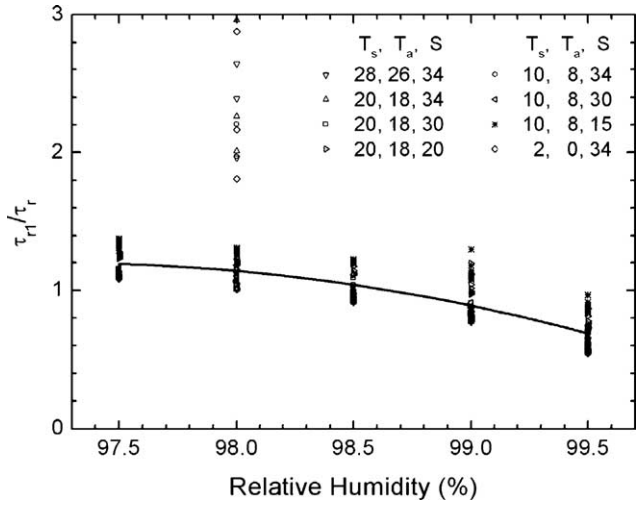

Fig. 10. Estimates of the radius e-folding time for high relative humidity that are based on Eq. (6.10) (i.e., τ_{rl}) are compared with estimates from the full microphysical model (i.e., τ_r). The plot shows computations for 13 initial radii (r_0) between 0.5 and 500 μm (not distinguished on the plot) for each of eight combinations of sea surface temperature (T_s, in °C), air temperature (T_a, in °C), and surface salinity (S, in psu). The barometric pressure is always 1000 mbar. The line is Eq. (6.11).

Fig. 10, however, suggests that Eq. (6.10) does not compare well at high humidities with values of τ_r from the full microphysical model. This plot compares estimates of τ_r from Eq. (6.10) and from the full microphysical model for eight combinations of surface temperature, air temperature, and surface salinity. Further, for each combination of conditions, I estimate τ_r for five relative humidities and for 13 initial droplet radii ranging from 0.5 to 500 μm. The plot includes all 520 of these comparisons of τ_r. In other words, the cluster of points at each relative humidity has 104 members.

The few outliers at RH=98% in Fig. 10 arise because my full microphysical model for radius evolution, Eq. (2.1), has some trouble when $f-1-y$ is near zero early in the calculation: that is, when the droplets starts near equilibrium. This is the situation when RH=98% and S=34 psu.

The solid line in Fig. 10 is

$$\tau_{rl}/\tau_r = -9.4013\times10^2 + 1.93607\times10^3 f - 9.955\times10^2 f^2, \tag{6.11}$$

where f is again the fractional relative humidity. This line is a reasonable fit to the averages of the points at each relative humidity depicted in Fig. 10 and, therefore, provides a correction to Eq. (6.10) for 97.5%≤RH≤99.5%. That is, an alternative estimate of τ_r when Eq. (6.8) fails at high humidity is

$$\tau_{r,est} = -\frac{r_0 - r_{eq}}{dr/dt|_{r_0}}\left(-9.4013\times10^2 + 1.93607\times10^3 f - 9.955\times10^2 f^2\right)^{-1}. \tag{6.12}$$

From the range of points shown in Fig. 10, we see that, for relative humidities between 97.5% and 99.5%, Eq. (6.12) has an accuracy comparable to the estimates shown in Figs. 8 and 9; it gives τ_r usually to within $\pm 20\%$.

7. Discussion

As I explained in the Introduction, my main motivation for developing quick estimates for T_{eq}, r_{eq}, τ_T, and τ_r is to use these in estimating the spray heat fluxes with equations such as Eqs. (1.1) and (1.2). Now, rather than having to use a full microphysical model to compute these microphysical endpoints, as Andreas (1992) and Andreas and DeCosmo (2002) did, I can estimate the spray-mediated heat fluxes roughly two orders of magnitude faster using the results of the last four sections.

Because Eq. (1.4) is an accurate model for the temperature evolution of a spray droplet until it starts undergoing significant evaporation or condensation, and because Eq. (1.6) is an accurate depiction for the evolution of an evaporating or condensing droplet, we can easily represent both processes using the quick estimates of T_{eq}, τ_T, r_{eq}, and τ_r. Fig. 11 again shows Fig. 1, but here I have added estimates of $T(t)$ and $r(t)$ from the exponential relations (1.4) and (1.6), respectively, and with T_{eq}, τ_T, r_{eq}, and τ_r calculated from the approximation formulas that I have presented.

In the figure for a time up to about 20 s, the exponential temperature approximation is virtually inseparable from the temperature evolution predicted by the full microphysical simulation. Clearly, the approximations for T_{eq} and τ_T that I have presented are very good.

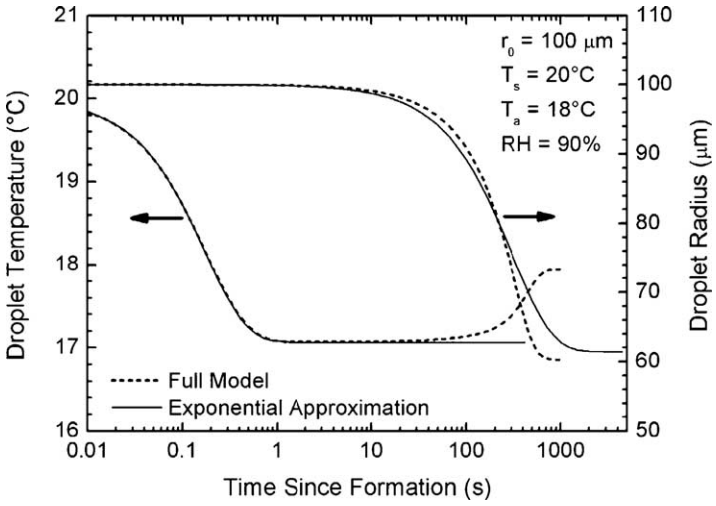

Fig. 11. Same as Fig. 1; but this plot also includes models of droplet evolution based on the exponential relations (1.4) and (1.6), with T_{eq} (=17.07 °C), r_{eq} (=61.44 μm), τ_T (=0.176 s), and τ_r (=303 s) calculated using the approximations developed here.

The exponential approximation for radius evolution in Fig. 11 is also good. In particular, the approximation for the equilibrium radius, r_{eq}, is within a micrometer of the value resulting from the full microphysical model. With the exponential approximation for radius evolution, however, the droplet radius is biased somewhat low early in the evolution and is biased high late in the evolution. This latter bias results, at least in part, because the approximation for the radius e-folding time τ_r tends to be too large; that is, the approximation predicts slower evolution than evidenced in the full microphysical model. Figs. 8 and 9 confirm this result. Both show that $\tau_{r,est}/\tau_r$ tends to be larger than one.

The late bias in the exponential approximation for radius also results because the exponential approximation for temperature does not capture the droplet's warming as the evaporation rate slows. Because the droplet warms above the T_{eq} value used to predict r_{eq} and τ_r, it exchanges vapor more quickly than if it were still at T_{eq} and thus reaches its equilibrium radius sooner than the exponential approximation predicts.

Fig. 11 suggests that the exponential approximations (1.4) and (1.6) have much larger ranges over which they are useful than the ranges I cited in the Introduction (based on Andreas, 1989). Taking Fig. 11 as representative, I conclude that Eq. (1.4) is an accurate model for droplet temperature for t/τ_T up to at least 100. Likewise, Eq. (1.6) is a reasonable model for droplet radius evolution all the way up to $r(t)=r_{eq}$, which is approximately true at $t/\tau_r=5$.

As a reality check, Andreas (1989, 1990) compared calculations from the full microphysical model with laboratory data for droplet evaporation from El Golli et al. (1974). Unfortunately, two of the three data sets from El Golli et al. that I had used were for very low relative humidities, 29% and 32%. As I explained, saline droplets eventually

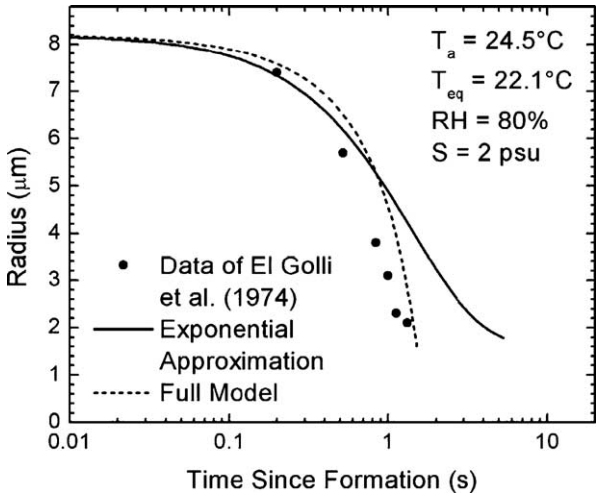

Fig. 12. Laboratory data from El Golli et al. (1974) show the evaporation of droplets with an initial radius of 8.2 μm. Values reported for the droplet equilibrium temperature (T_{eq}), relative humidity (RH), and initial salinity of the droplets (S) are listed. I infer the ambient air temperature (T_a) from these conditions. The lines show radius evolution predicted with my full microphysical model and with the exponential approximation (1.6), where I computed T_{eq}, r_{eq}, and τ_r from my approximation formulas.

undergo a phase transition to a salt crystal when they evaporate in such humidity. None of my approximation formulas recognize the possibility for such a transition and, therefore, cannot predict the microphysical endpoints in low humidities.

Fig. 12 does, however, show one of the El Golli et al. (1974) data sets with a more marine-like relative humidity, 80%. The data points here represent the evaporation of droplets with initial radius 8.2 μm and with initial salinity 2 psu. I infer from the droplet equilibrium temperature (22.1 °C) and the relative humidity (80%) that El Golli et al. report that the air temperature in their chamber was 24.5 °C.

Fig. 12 shows the exponential approximation for radius evolution, Eq. (1.6), where I have used the approximation formulas for T_{eq}, r_{eq}, and τ_r to calculate $r(t)$. The agreement with the data here is not as good as it is with the full microphysical model, which Fig. 12 also shows (cf. Andreas, 1989, 1990). For example, τ_r is again computed to be too large; hence, the exponential approximation predicts a radius evolution that is too slow. Still, the approximation predicts that the evolution reaches the last observed radius point, 2.1 μm, at 3.6 s, only 2.4 s slower than the observed time. In some applications, estimates with this accuracy may be good enough.

8. Summary

Because both the temperature and the radius of saline droplets evolve with time following approximately exponential relations–namely, Eqs. (1.4) and (1.6)–that evolution can be represented with only four so-called microphysical endpoints: T_{eq}, τ_T, r_{eq}, and τ_r. These are, respectively, the droplet's equilibrium temperature and the e-folding time to reach that temperature and the droplet's equilibrium radius and the e-folding time to reach that radius. Full microphysical simulations of droplet evolution yield these endpoints, but often we would like quicker estimates that are not as computationally intensive to obtain.

Therefore, starting with the microphysical equations for droplet temperature and radius, I have derived quick approximation formulas for all four of these endpoints. The fact that the temperature evolution and the radius evolution of small, saline droplets are largely decoupled underlies the success of the approximations. In effect, I can assume that the droplet radius is constant at its initial value r_0 during the temperature evolution and that the droplet temperature is constant at T_{eq} during most of the radius evolution. The resulting equations for estimating T_{eq}, τ_T, and τ_r involve one-step calculations; finding r_{eq} requires an iteration based on Newton's method.

Several examples that compare these approximate methods with values of T_{eq}, τ_T, r_{eq}, and τ_r from a full microphysical simulation demonstrate the validity of the approximation methods. That is, my quick estimates of T_{eq} are typically within 0.02 °C of temperatures computed in a full microphysical simulation (cf. Andreas, 1996). Quick estimates of the temperature e-folding time τ_T are typically within 5% of e-folding times that come from the full model. Fig. 11 further demonstrates how good these estimates of temperature endpoints are and how useful the exponential approximation for temperature evolution, Eq. (1.4), is. That figure shows that Eq. (1.4) predicts a temperature evolution that is virtually indistinguishable from the temperature evolution predicted by the full microphysical model for t/τ_T out to 100.

My approximation formulas for the equilibrium radius r_{eq} also produce very good results when compared to the full microphysical model. These quick estimates of r_{eq} are typically within 5% of results from the full model. The radius e-folding time, τ_r, however proved the most difficult quantity to estimate quickly. Some of my estimates of τ_r exceed times based on a full microphysical simulation by 25%. For typical oceanic conditions, however–with a surface salinity near 34 psu and with near-surface relative humidities of a least 80%–the estimates of τ_r are better. They are typically within 10% of values from the full model.

In closing, though I have concentrated here on saline droplets, the microphysical equations are capable of forecasting the evolution of aqueous solution droplets containing a variety of solutes. With minor modifications to these equations to adapt them for solutes other than NaCl, I see no reason why my approximation formulas would not also be able to predict the microphysical endpoints for a variety of other solution droplets.

Symbols

a	(=17.502) constant occurring in Buck's (1981) equation for saturation vapor pressure
A	variable used in approximating droplet temperature evolution; see Eq. (4.6)
b	(=240.97 °C) constant occurring in Buck's (1981) equation for saturation vapor pressure
B	variable used in approximating droplet temperature evolution; see Eq. (4.7)
c_{ps}	(=4000 J kg^{-1} K^{-1}) specific heat of seawater at constant pressure
dF/dr_0	spray generation function in terms of r_0
D_w	molecular diffusivity of water vapor in air
D'_w	water vapor diffusivity modified for noncontinuum effects
e_{sat}	saturation vapor pressure
f	fractional relative humidity (i.e., f=RH/100)
$g(r)$	function used to estimate a droplet's equilibrium radius; see Eq. (5.2)
h	function that models the evolution of the nondimensional droplet radius; see Eq. (6.1)
k_a	thermal conductivity of air
k'_a	thermal conductivity modified for noncontinuum effects
L_v	latent heat of vaporization of water
m	molality of a spray droplet; see Eq. (2.4)
m_s	mass of salt in a spray droplet
M_s	(=58.443 × 10^{-3} kg mol^{-1}) molecular weight of sodium chloride
m_w	mass of pure water in a spray droplet
m_{w0}	initial mass of pure water in a spray droplet
M_w	(=18.015 × 10^{-3} kg mol^{-1}) molecular weight of water
Q_L	air–sea latent heat flux mediated by spray
Q_s	air–sea sensible heat flux mediated by spray
r	[or $r(t)$] instantaneous spray droplet radius
R	(=8.31447 J mol^{-1} K^{-1}) universal gas constant
r_d	effective dry radius of a sea salt particle

r_{eq}	equilibrium radius of a spray droplet
$r_{eq,est}$	quick estimate of a droplet's equilibrium radius r_{eq} from Eqs. (5.1)–(5.4)
$r_{eq,F}$	estimate of a droplet's equilibrium radius r_{eq} based on Fitzgerald's (1975) algorithm
RH	ambient relative humidity in percent
r_k	kth recursive estimate of r_{eq}; see Eq. (5.3)
r_0	initial radius of a spray droplet
s	fractional salinity (i.e., $s = S/1000$)
S	salinity in practical salinity units (psu, which is practically parts per thousand by mass, ‰)
t	time
T	[or $T(t)$] instantaneous spray droplet temperature
T_a	ambient air temperature
T_{eq}	equilibrium temperature of a spray droplet
$T_{eq,est}$	quick estimate of a droplet's equilibrium temperature from Eqs. (3.1)–(3.4)
T_s	sea surface temperature (also initial temperature of the spray droplets)
T_{wet}	classical wet-bulb temperature
y	variable that accounts for curvature and salinity effects on the surface vapor pressure of a spray droplet; see Eqs. (2.2) and (2.8)
α	dimensionless variable used to estimate a droplet's equilibrium temperature; see Eq. (3.2)
β	variable used to estimate a droplet's equilibrium temperature; see Eq. (3.3)
ΔT	$T_{eq,est} - T_a$; see Eq. (3.4)
v	(=2) number of ions into which a sodium chloride molecule dissociates
ρ_{NaCl}	($=2.165 \times 10^3$ kg m^{-3}) density of sodium chloride
ρ_s	density of seawater
ρ_v	ambient water vapor density
ρ_{vr}	water vapor density at the surface of a spray droplet
$\rho_{v,sat}$	saturation water vapor density
ρ_w	density of pure water
σ_s	surface tension of a flat water surface with temperature T and salinity S
τ_f	residence time in air of a spray droplet (parameterized in terms of its terminal fall speed)
τ_r	droplet radius e-folding time
$\tau_{r,est}$	quick estimate of droplet radius e-folding time τ_r; see Eqs. (6.8) and (6.12)
τ_{r1}	quick estimate of droplet radius e-folding time τ_r based on a first-order estimate; see Eq. (6.10)
τ_T	droplet temperature e-folding time
$\tau_{T,est}$	quick estimate of droplet temperature e-folding time τ_T; see Eq. (4.11)
Φ_s	practical osmotic coefficient of sodium chloride dissolved in water; see Eq. (2.3)

Acknowledgements

I thank two anonymous reviewers for helpful comments. The U.S. Office of Naval Research supported this work with awards N0001404MP20091 and N0001405MP20044.

References

Andreas, E.L, 1989. Thermal and Size Evolution of Sea Spray Droplets. CRREL Report 89-11. U.S. Army Cold Regions Research and Engineering Laboratory, Hanover, N.H. 37 pp.
Andreas, E.L, 1990. Time constants for the evolution of sea spray droplets. Tellus, 42B, 481–497.
Andreas, E.L, 1992. Sea spray and the turbulent air–sea heat fluxes. J. Geophys. Res. 97, 11429–11441.
Andreas, E.L, 1995. The temperature of evaporating sea spray droplets. J. Atmos. Sci. 52, 852–862.
Andreas, E.L, 1996. Reply. J. Atmos. Sci. 53, 1642–1645.
Andreas, E.L, 2002. A review of the sea spray generation function for the open ocean. In: Perrie, W. (Ed.), Atmosphere-Ocean Interactions, vol. 1. WIT Press, Southampton, U.K., pp. 1–46.
Andreas, E.L, 2004. Spray stress revisited. J. Phys. Oceanogr. 34, 1429–1440.
Andreas, E.L, Cash, B.A., 1996. A new formulation for the Bowen ratio over saturated surfaces. J. Appl. Meteorol. 35, 1279–1289.
Andreas, E.L, DeCosmo, J., 1999. Sea spray production and influence on air–sea heat and moisture fluxes over the open ocean. In: Geernaert, G.L. (Ed.), Air–Sea Exchange: Physics, Chemistry and Dynamics. Kluwer, Dordrecht, pp. 327–362.
Andreas, E.L, DeCosmo, J., 2002. The signature of sea spray in the HEXOS turbulent heat flux data. Boundary-Layer Meteorol. 103, 303–333.
Andreas, E.L, Emanuel, K.A., 2001. Effects of sea spray on tropical cyclone intensity. J. Atmos. Sci. 58, 3741–3751.
Bao, J.-W., Wilczak, J.M., Choi, J.-K., Kantha, L.H., 2000. Numerical simulations of air–sea interaction under high wind conditions using a coupled model: a study of hurricane development. Mon. Weather Rev. 128, 2190–2210.
Buck, A.L., 1981. New equations for computing vapor pressure and enhancement factor. J. Appl. Meteorol. 20, 1527–1532.
Edson, J.B., Fairall, C.W., 1994. Spray droplet modeling: 1. Lagrangian model simulation of the turbulent transport of evaporating droplets. J. Geophys. Res. 99, 25295–25311.
Edson, J.B., Anquentin, S., Mestayer, P.G., Sini, J.F., 1996. Spray droplet modeling: 2. An interactive Eulerian-Lagrangian model of evaporating spray droplets. J. Geophys. Res. 101, 1279–1293.
El Golli, S., Bricard, J., Turpin, P.-Y., Treiner, C., 1974. The evaporation of saline droplets. J. Aerosol Sci. 5, 273–292.
Fairall, C.W., Kepert, J.D., Holland, G.J., 1994. The effect of sea spray on surface energy transports over the ocean. Global Atmos. Ocean Syst. 2, 121–142.
Fitzgerald, J.W., 1975. Approximation formulas for the equilibrium size of an aerosol particle as a function of its dry size and composition and the ambient relative humidity. J. Appl. Meteorol. 14, 1044–1049.
Kepert, J.D., 1996. Comments on "The temperature of evaporating sea spray droplets". J. Atmos. Sci. 53, 1634–1641.
Kepert, J.D., Fairall, C.W., Bao, J.-W., 1999. Modelling the interaction between the atmospheric boundary layer and evaporating sea spray droplets. In: Geernaert, G.L. (Ed.), Air–Sea Exchange: Physics, Chemistry and Dynamics. Kluwer, Dordrecht, pp. 363–409.
Kinzer, G.D., Gunn, R., 1951. The evaporation, temperature and thermal relaxation-time of freely falling water drops. J. Meteorol. 8, 71–83.
Lighthill, J., 1999. Ocean spray and the thermodynamics of tropical cyclones. J. Eng. Math. 35, 11–42.
Pattison, M.J., Belcher, S.E., 1999. Production rates of sea-spray droplets. J. Geophys. Res. 104, 18397–18407.
Pruppacher, H.R., Klett, J.D., 1978. Microphysics of Clouds and Precipitation. D. Reidel, Dordrecht. 714 pp.
Twomey, S., 1953. The identification of individual hygroscopic particles in the atmosphere by a phase-transition method. J. Appl. Phys. 24, 1099–1102.
Van Eijk, A.M.J., Tranchant, B.S., Mestayer, P.G., 2001. SeaCluse: numerical simulation of evaporating sea spray droplets. J. Geophys. Res. 106, 2573–2588.